

XMM Flight Mirror Modules with Reflection Grating Assembly and X-Ray Baffle Testing

Y. Stockman, I. Domken, H. Hansen, J. Ph. Tock

CSL – University of Liège

B- 4031 Angleur, Belgium

email : ystockman@ulg.ac.be

T.A. Decker, A. Rasmussen

Columbia University, 538W. 120th Street New York, NY 10027, USA

A.J.F. den Boggende, J.W. den Herder, F. Paerels

SRON, Sorbonnelaan 2, 3584 C.A. Utrecht, The Netherlands

G. Bagnasco, D. de Chambure, C. Erd, Ph. Gondoin

ESA / ESTEC

PO BOX 299, 2200 AG Noordwijk, The Netherlands

ABSTRACT

In the frame of the XMM project, several test campaigns are accomplished to qualify the optical elements of the mission. The tests described in this paper are performed on a XMM Flight Model Mirror Module (FM MM) added with a Reflection Grating Assembly (RGA). The Mirror Module contains 58 X-ray optical quality shells, an X-ray baffle (XRB) to reduce the straylight. This complete XMM Flight Model Mirror Assembly (MA) is tested in a vertical configuration at CSL, in a full aperture or partial EUV collimated beam illumination, and with an X-ray pencil beam. One of the advantages of the EUV collimated beam is to verify the correct position of the RGA when integrated in flight configuration on the Mirror Module structure. This is not possible in X-ray with a finite source distance. The partial EUV illumination is performed to verify the correct integration of the RGA grating stacks. The pencil beam allows to make an accurate metrology of the XRB position, and to verify the positions of the 0, 1 and 2 diffraction order foci.

In this paper, the tested module is first exposed, and the approach to qualify the instrument is described. The analysis of the results achieved over the different test configurations is presented. The impact of the environmental tests on the Reflection Grating Box is also diagnosed.

KEYWORDS :

X-ray optics and telescope, EUV optics, test facility, XMM

1. INTRODUCTION

The X-ray Multi Mirror Mission ^{1,2,3} (XMM) due for launch in August 1999, by ARIANE 5, has been designed to be a high throughput spectroscopy mission over a broad energy band ranging from 0.1 to 12 keV. The payload includes :

- three co-aligned grazing incidence telescopes made of 58 nested Wolter I mirror shells (MS)
- three imaging EPIC cameras (European Photon Imaging Camera)
- two Reflecting Grating Assemblies (RGA) put immediately behind two of the three Mirror Modules (MM)
- two RGA Focal plane Camera's (RFC's) located at the first order focus of the RGA
- three X-ray Baffles (XRB) put in front of each MM

Up to now, four stand-alone Flight Model Mirror Modules (FM1 to 4 MMs) have been manufactured and tested^{4,5}. An XRB must be integrated on each of them. Based on the results of the calibration and environmental tests, three out of the four MMs will be selected to be integrated on the payload. Out of this three, two will be chosen to accommodate the RGA. Up to now, the four FM MMs have been tested separately at CSL. The two first FM MMs have been certified with the XRB integrated, and a check of the correct integration and good operation of the XRB has been performed⁴. The two FM RGAs have also

been tested in full and partial EUV collimated illumination using respectively FM1 MM and FM2 MM for FM1 RGA and FM2 RGA. This latter configuration includes also the mounting of the FM2 XRB, this means a complete optical flight configuration.

Engineering and calibration tests have been performed to verify the correct operation of the system. A flow chart test plan is presented in figure 1. Engineering tests are first performed to characterise the MM and to evaluate the impact of launch and orbit environmental conditions. The MM is submitted to X-ray calibration at the Panter facility¹². At this stage the XRB can not be integrated on the MM because of the geometry of the test configuration. This is performed at CSL. The results of the XRB manufacturing, integration, efficiency and the impact of the environmental test are reported in ref 4. Once this subsystem fully characterised the RGA is integrated on the MM. This system is exposed to an EUV collimated full illumination, that allows to verify the correct alignment with respect to the MM and image quality at the various foci (telescope and 0-order diffraction). In a second engineering test campaign the MM with the RGA is partially illuminated by an EUV collimated beam that permits to check the correct alignment of each elementary grating stack with respect to each other. A last test consists in X-ray illumination to check the first and second diffraction order, and the efficiency of a selected grating.

This paper is describing these later experiments performed on these last test configurations and the achieved results. It is also presenting the environmental tests performed on the RGA FM2 alone.

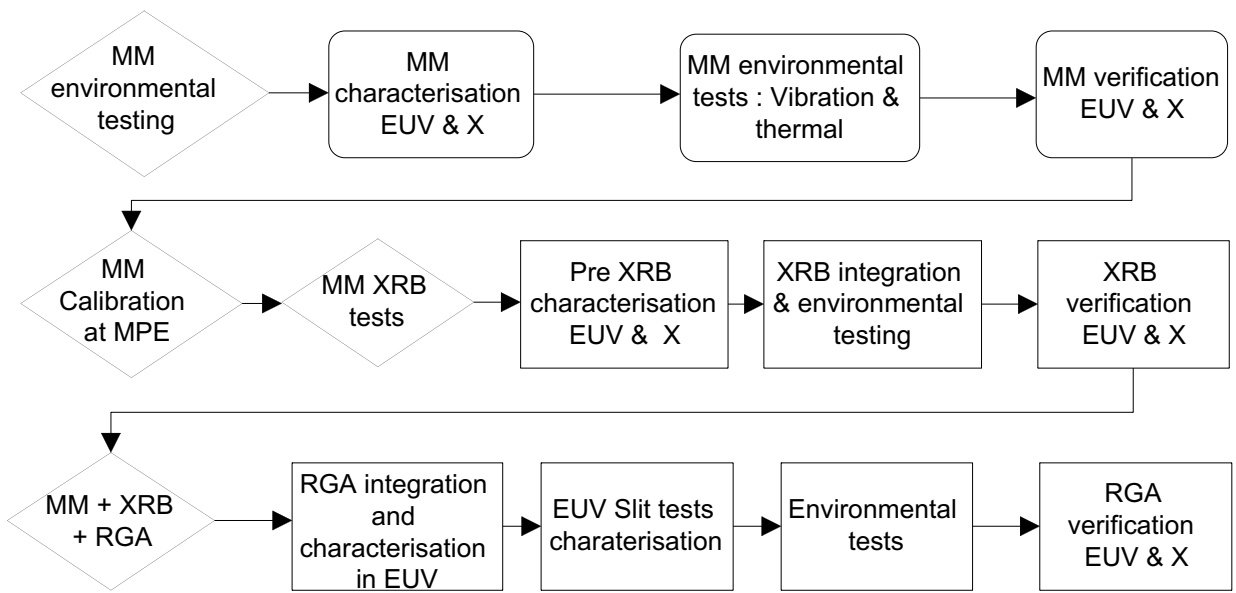


Figure 1 : Mirror Module test plan

2. EUV EXPERIMENTAL SET-UP

2.1. Introduction

The aim of the Extreme Ultra Violet (EUV) collimated illumination is to simulate a star without being limited by diffraction. The set-up has been built vertically to minimise the gravity effect on the very thin mirrors and on their supporting structure. The combination of these two concepts allows to test any MM in a configuration close to in-flight operation, this is still true when a RGA is added. The main drawback is the use of EUV light that is not in the instrument working energies and by this way the first and second diffraction order of RGA can not be observed. This collimator is used for more than 2 years and has already tested 5 MMs, including pre and post environmental optical tests, XRB integration and RGA tests. This represents about 807 working days of 8 hours! This EUV channel allows to measure the Point Spread Function (PSF) at nominal focus, at best focus, at zero order grating foci on axis and within the Field Of View (FOV). This configuration has also been used to verify the correct design of the XRB thanks to straylight measurements⁴.

2.2. Set-up description

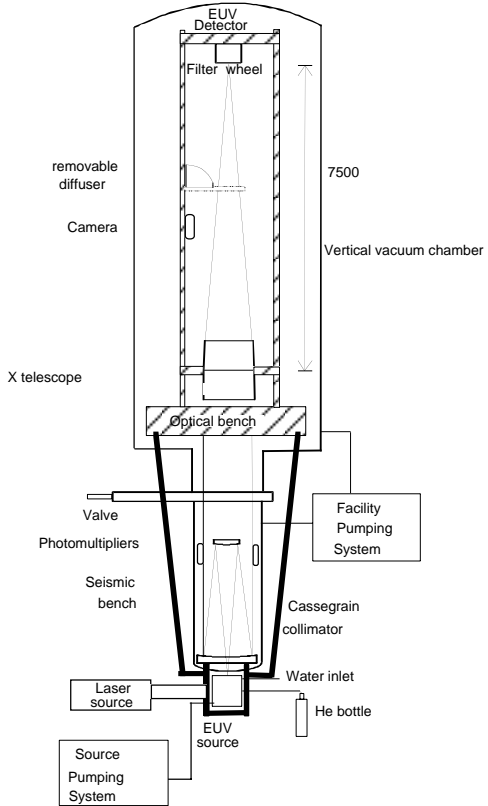


Figure 2 : EUV channel general layout

This set-up has been largely described in ref. 6,7, and consists mainly in a 12 m height and 4.5 m diameter test chamber. The EUV source installed in the 15 m depth pit is an Electron Cyclotron Resonance providing He lines at 58.4 and 30.4 nm. The source illuminates a Φ 800 mm Cassegrain collimator through a 100 μm diameter pinhole. This collimated beam is focalised by the telescope on a thinned back side illuminated CCD through a meshless Al filter, rejecting all the visible light of the source. The CCD has 770 * 1152 pixels of 22.5 * 22.5 μm_size . This is equivalent to 12 * 8 arcmin XMM field of view with a resolution of 0.6 arcsec. A general layout of the EUV channel is shown in figure 2. A visible source (10 mW HeNe laser) is used for alignment purposes. The pinhole of the laser spatial filter is placed at a conjugate focal point of the collimator by means of a removable mirror. The use of the visible light allows to predetermine the critical positions (e.g. nominal telescope focus, zero order grating focus, partial illumination positions, ...). All the optical parts, telescope included, are on a rigid optical bench, fixed on a seismic block. The feet tightness is realised by bellows that isolate the optical bench from ground and pumping system vibrations. Since, it has been observed that the source position in front of the pinhole influences the collimator homogeneity, the homogeneity is controlled by four photomultipliers. In a command room two work stations manage the facility, one mainly for temperature and pressure control and displacements, and a second one for image acquisition and data handling. Analyses are carried out on site, using homemade software both on-line and off line.

3. XRB INTEGRATION AND TESTS

X-Ray Baffle⁸ (XRB) has been introduced to reduce off axis straylight coming from X-ray sources between 0.5 and 1.4°. For these illumination angles, single reflection on the hyperbola mirrors goes straight in the EPIC area. To decrease this straylight the idea is to reduce the access to these hyperbola mirrors. This is achieved by a “pre-collimator” (or X-ray baffle) consisting of thin cylindrical shells which extend the mirror shells forward. In order to reduce reflection and scattering from the cylindrical surfaces, cylindrical sections can be removed leaving thin circular annular rings in front of each mirror. They are carefully aligned in front of the annular aperture of the 58 MSs. It has already been presented and demonstrated that the integration and the design of the X-ray baffle are correctly performed⁴.

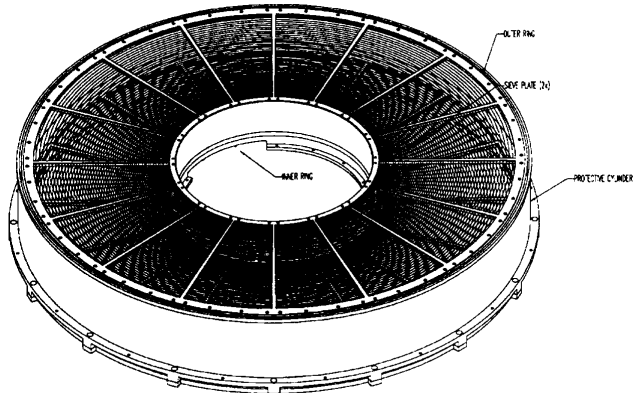


Figure 3 : X-ray baffle 3-D view

The integration and verification sequence is the following :

- Determination of the MSs position following 4 orthogonal azimuths, before and after integration and check if there is no difference.
- Verification that the image quality is not degraded.
- Verification that there is no modification of the effective area on axis.

- Comparison of the experimental Field Of View (FOV) vignetting function with the modelled one.
- Verification that the straylight is correctly reduced between 30 and 90 arcmin.

All these tests have been conducted successfully at CSL. Environmental tests consisting in vibration and thermal cycling tests have also been performed. It has been demonstrated⁴ that these environmental tests have no impact on the integration neither on the XRB integrity and efficiency.

4. REFLECTION GRATING ASSEMBLY

When the XRB is mounted 85 mm in front of the entrance plane, the RGA is installed in the converging telescope beam at about 500 mm from the MS exit plane. The RGA consists^{9,10} of a main structure made of Beryllium. This structure supports about 200 identical diffraction gratings of 10 by 20 cm size. Each of these gratings is oriented so that it diffracts the beam on a common point on the Rowland circle. At this location nine large format backside illuminated CCDs operating in counting mode are used for spectroscopy analysis. This camera is called the RFC (RGA Focal plane Camera). The gratings stacks pick off about half of the outgoing beam of the MM, and deflect it to the RFC. The other half goes through the RGA and focalises on EPIC detector (European Photon Integration Counter), situated on the Rowland circle, at the telescope focus. All the structure is interfaced to the MM RGA interface via three Titanium feet. These feet have a particular design⁹ to reduce the stress transfer into the structure during the launch. Shims can be added to fit the actual focal length of each MM.

At the centre of the RGA a Central Alignment Mirror (CAM) is used to align the RGA with respect to MM alignment lens optical axis. The Cam orientation with respect to the general orientation of the gratings is measured during grating stacks integration. Presently two RGA have been manufactured and tested at CSL. The tests realised on each RGA are slightly different and will be presented hereafter.

5. RGA FM2 ENVIRONMENTAL TESTS

The FM2 RGA has been submitted independently to thermal and vibration tests. The thermal test has been conducted in FOCAL 3 (Facility for Optical Calibration at Liège). This cylindrical chamber is three meter high and three meter in diameter. The RGA is surrounded by a thermal tent composed of 6 copper panels fixed on an aluminium structure. Six thermal cycles ranging from +10°C (cold case) to + 30°C (hot case) have been applied. This corresponds to the operating and non-operating temperature range. One thermal cycle takes about 18 h, the shroud gradient is limited to 0.5°C/min. The thermal test began by a cold case and after the six cycles, the shrouds temperature set points have been set to 15°C in order to keep the RGA2 warmer than the shrouds during return to room temperature.

After this thermal cycling the RGA2 was transferred to the shaker facility. This one consists in a long stroke electrodynamic shaker (Ling Electronics Model 2016-U). The RGA2 is submitted to sinusoidal and random vibration along the X (optical axis), Y and Z direction at equivalent ARIANE 5 levels. The levels are : 10 g along axial X axis and 5.33 g along lateral Y, Z axis. Good correlation with the numerical model is observed.

This environmental tests sequence took place in between two full illumination optical tests. The aim of these optical tests was to assess the impact of environmental tests on the optical performances.

6. EUV FULL ILLUMINATION MEASUREMENTS

6.1 Introduction

The XRB FM2 has been integrated on the FM2 MM. Dedicated tests have been performed on this subsystem, confirming the good image quality of the MM but also the good integration and performance of the XRB. This subsystem has passed the environmental tests with success^{4,5}. The RGA2 was integrated on this MM FM2 entity. The RGA2 is aligned with the help of

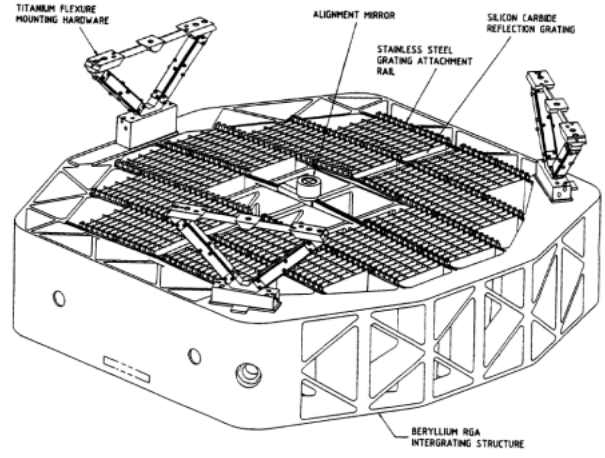


Figure 4 : RGA 3-D view

the MM alignment lens and the RGA alignment lens. All these activities are performed in a class 100 clean room environment before the introduction of the complete system in the main chamber. Since the mechanical axis is used during spacecraft integration, the complete MM mechanical axis is aligned with respect to the collimator optical axis. This is realised using :

- The alignment lens positions with respect to the EUV determined on the FM2 MM + XRB just before the RGA integration. This is required because the MM alignment lens is not more accessible from the top once the RGA is integrated.
- Second the measurement of the alignment lens with respect to the mechanical axis. This is performed using theodolites.
- From the previous results tilt adjustments are performed to achieve the final alignment.

6.2 PSF Measurements at 58.4 nm

Once the MM is correctly aligned, a best focus search is performed by stepping along the optical axis by steps of 2 mm. The radial HEW is measured each step. This is done for the telescope focus and for the 0-order focus. The range of this scan is 40 mm around the nominal focus with some points up to 160 mm. The introduction of the RGA doesn't change the telescope focal length. Around the 0-order focus, the PSF can be measured on the Rowland circle, at best dispersion focus, at best cross dispersion focus and at best radial focus. The plots of figure 5 shows the focal depth for EPIC and 0-order foci in dispersion and cross dispersion direction. The PSF best focus images at EPIC and 0-order positions are presented in figure 6. The telescope best focus is to be compared to the best focus when the RGA is not integrated. The presence of the RGA changes slightly the image quality. This is confirmed by the values of Half Energy Width (HEW) and Full Width at Half Maximum (FWHM). This minor effect is due to the diffraction introduced by the RGA. For FM1 MM and RGA1 the differences are larger. The reason is that the MM was not correctly aligned with respect to the collimated beam. This mis alignment is due to an alignment lens problem.

Accurate observation of the 0-order focus shows that there is a slight change between image before and after environmental test with FM2. The tail going along $-Z$ is decreasing, and the HEW decreases by two arcsec. Explanation of this improvement is provided by the analysis of the extrafocal images (see next paragraph). For EPIC focus there is no observed impact of the environmental test on the image quality.

Table 1 : HEW, 90EW and FWHM computed at best focus for FM MM1 and 2 with and without RGA1 and RGA2

Test campaign [arcsec]	FM1 MM	FM1 + RGA1	FM1 + RGA1 0-order Foc	FM2 MM	FM2 + RGA2 EPIC Foc	FM2 + RGA2 0-order Foc
HEW	15.5	16.5	28.2	15.4	16.1	23.4
90EW	62.6	63.9	83.7	62.5	66.7	71.5
FWHM	6.7	7.2	18.0	6.3	6.7	16.1

Figure 5: Best focus curves. The left one (5.a) is the best focus fitting for EPIC focus. The right one (5.b) is the best focus fitting for the 0-order diffraction. The ordinates are in arcsec in HEW and the abscissas are in CSL μm detector coordinates.

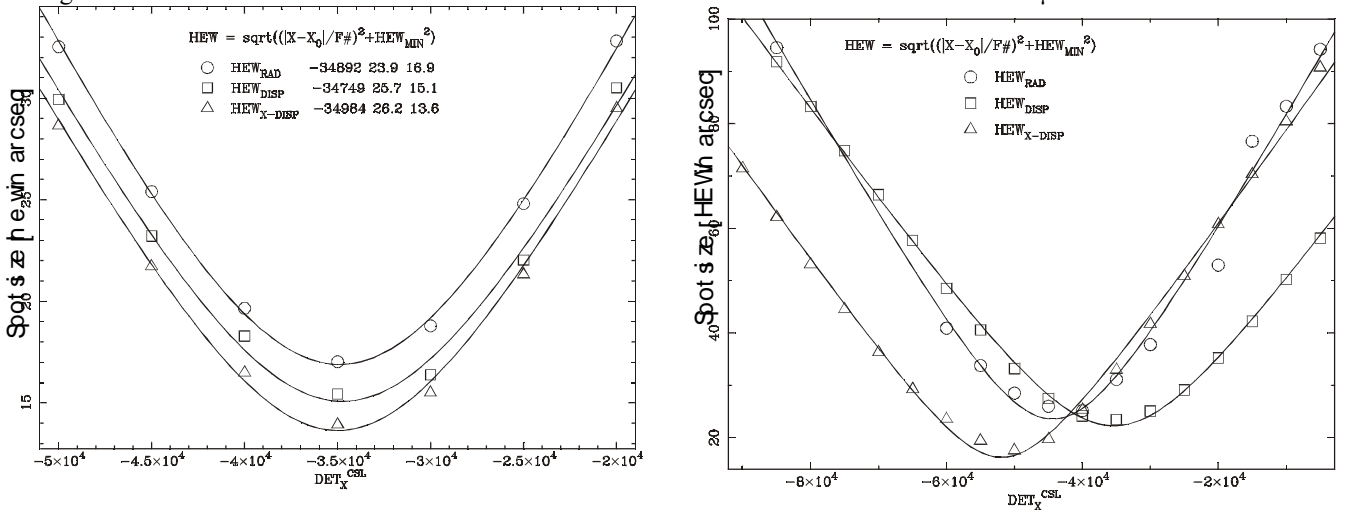


Figure 6: 2D view in log scale of the best focus PSF at EPIC and 0-order foci positions with 58.4 nm radiation.
The images are normalised to the maximum signal. The ratio between two adjacent iso contour is 1.6.

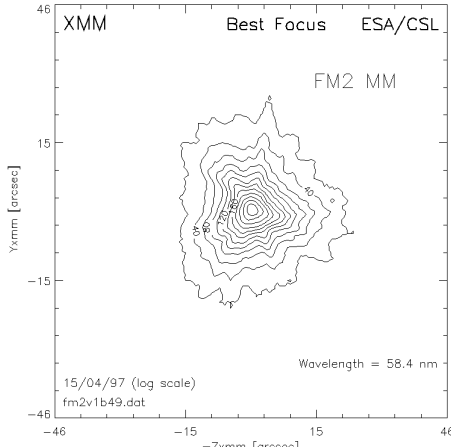


Figure 6.a : FM2 Best focus at Epic without RGA

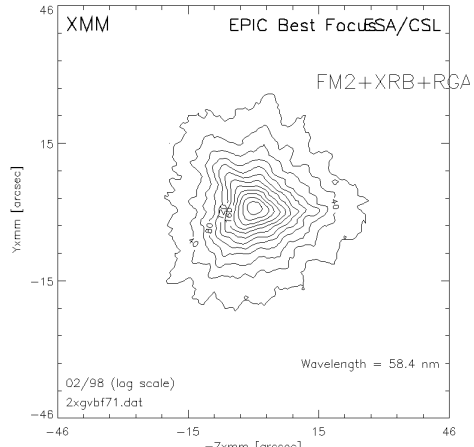


Figure 6.b. : FM2 MM Best focus at Epic with RGA

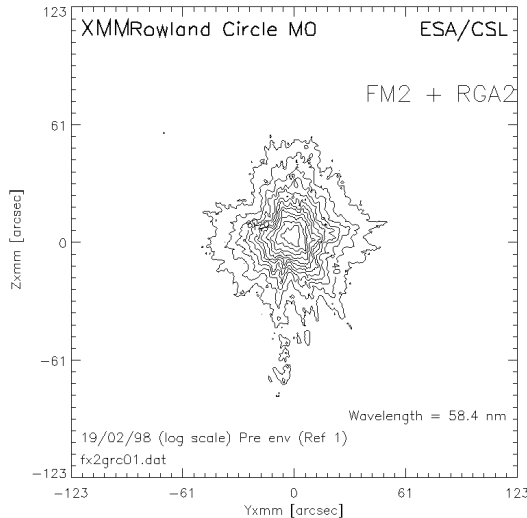


Figure 6.c : FM2 Best focus at 0-order diffraction before environmental test

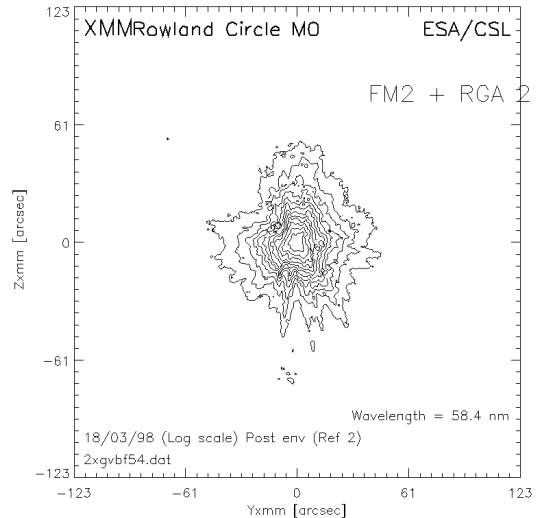


Figure 6.d : FM2 Best focus at 0-order diffraction after environmental test

6.3. Extrafocal images

The acquisition of extrafocal images is an other useful diagnostic tool. Due to the limited size of the facility CCD detector, the extrafocal images are built up by making a mosaic reconstruction. The images in figures 7.a. to 7.d are made of 6 CCD images. Due to hardware vignetting in front of the detector some parts of the image are missing (triangular shape near the centre of the 0-order extrafocal images). These images were taken at an extrafocal position of 350 mm from the EPIC nominal focus. The upper ones are for EPIC extrafocal image, with and without RGA2 on FM2 MM, when the lower ones are for the 0-order extrafocal images before and after environmental tests. For the figures 6.c and d, the - Z XMM coordinates points upward, that is also the grating dispersion axis, when the Y XMM points to the right. The vignetting effect introduces

by the integration of the RGA2 is obvious on the images of figure 7.b. compared to figure 7.a. The orientation of the grating stacks is easily observed.

For what concerns the 0-order extrafocal images, misaligned gratings are clearly detected, particularly the stacks T2-2 (lower left) and T4-6 (central up right). The impact of this misaligned stacks represents only 0.5 % in terms of energy. After the environmental tests the previously misaligned stack T4-6 is aligned, the T2-2 remains misaligned. This improvement in stack alignment due the environmental tests is the reason why the best focus PSF image quality improved also in terms of HEW and image shape (reduction of the -Z tail on figure 6.d).

Figure 7 : + 380 mm extra focal images composed of a mosaic of 6 CCD images of EPIC and 0-order.

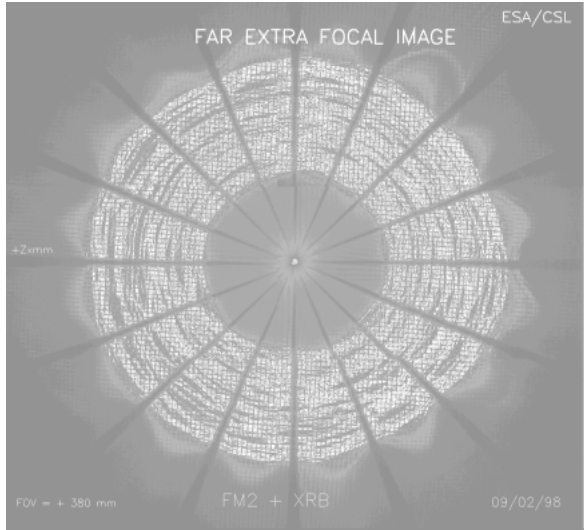


Figure 7.a : Extra focal image of FM2 MM without RGA2 EPIC focus



Figure 7.b : Extra focal image of FM2 MM with RGA2 EPIC focus

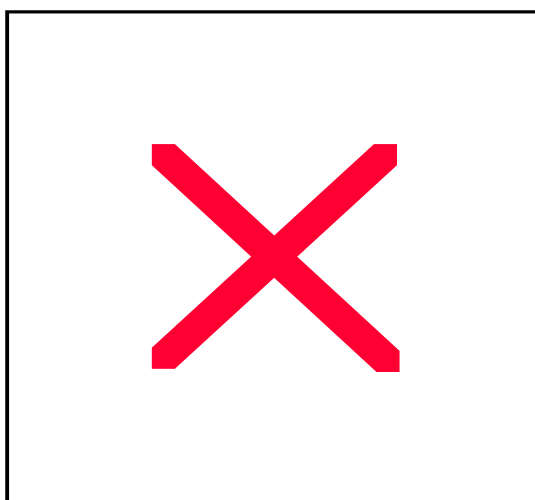


Figure 7.c : Extra focal image of FM2 MM with RGA2 EPIC focus

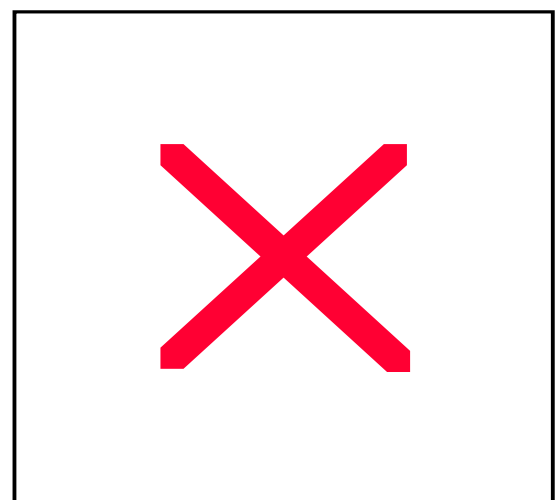


Figure 7.d : Extra focal image of FM2 MM with RGA2 at 0-order focus after environmental tests

The splitting of the effective area between EPIC (telescope focus) and 0-order diffraction focus has also been measured. This one is summarised in Table 2 and is compared to the geometric clear aperture fraction. The relative effective area at 0-order for a 58.4 nm radiation will be provided by the SCISIM model (the XMM software simulator). The measured values are 1% less than the expected ones. This is largely inside the accuracies.

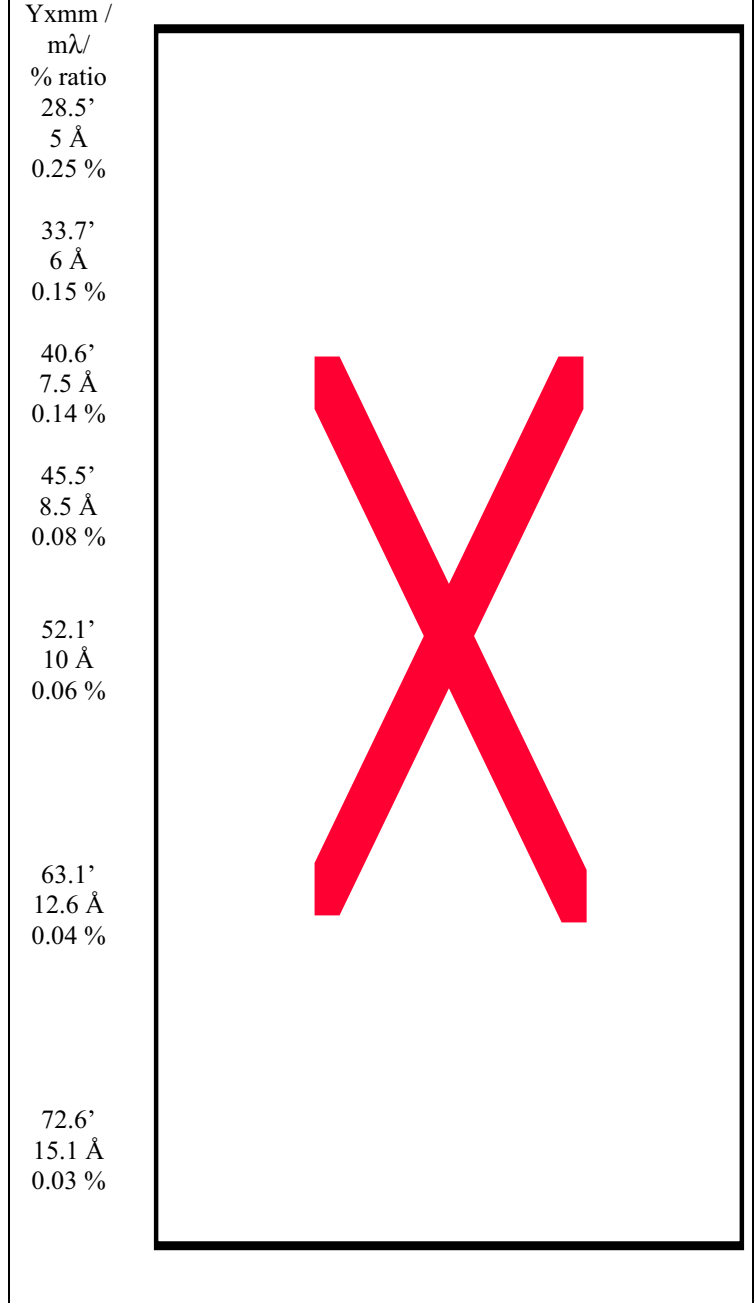
Table 2: Relative effective area splitting between EPIC focus and 0-order focus

Unit in %	Measured relative area	Theoretical relative area
EPIC focus	44 +/- 2	45 +/- 2
M=0	32 +/- 2	

6.4 Straylight tests

From theoretical straylight analysis, it has been demonstrated¹¹, that visible light diffracted by the 0-order grating reaches area where first order X-ray impinged the RGS detectors. To confirm these theoretical assumptions, a straylight test measurement has been performed. This one is realised in the same way as for straylight measurement⁴ on the MM alone. The whole optical bench is tilted, in such a way that the MM + RGA + facility detector tilts as an individual telescope in front of the EUV collimated beam. The facility CCD detector can then be translated to reach the interesting areas. These are the different diffraction orders, the source image focus or the EPIC telescope focus. The tilts were performed around Y_{XMM} at 28.5, 33.7, 40.6, 45.5, 52.1, 63.1, 72.6 arcmin, corresponding to the RGS position of 5, 6, 7.5, 8.5, 10, 12.6, 15.1 Å wavelengths for the actual configuration. The figure 8 represents the corresponding “focused stars” on the RGS camera. These images will be attenuated by rejection filter. To quantify the among of straylight flux, the flux in the straylight images is compared to the flux in EPIC for an on axis source. These ratios are expressed in %, in the first column of figure 8. This is a first and raw evaluation, since on several frames the image is vignetted.

Figure 8 : Straylight images on RGS for off axis “stars”. On the left, EUV focus point sources for off axis field angle of (from top to bottom) 28.5, 33.7, 40.6, 45.5, 52.1, 63.1, 72.6 arcmin. On the right, the diffuse light arriving on RGS for off axis angles of $Y_{\text{XMM}} = 14.2$ and 22.8 arcmin. These images are plotted in logarithmic scale and have not been normalised with respect to the incident beam. The third number in the first column is the normalised ratio with the on axis EPIC focus expressed in %. The aspect ratio of the mosaic is true, i.e. there is 96 mm between the upper left spot (5 Å position) and the lower position left spot (15.1 Å position).



7. FIRST AND SECOND ORDER DIFFRACTION

To check the correct operation of the RGA in X-rays, once integrated on the MM, and the correct position of the different diffraction orders, the MM with RGA has been illuminated by the pencil beam. The pencil beam is realised with two pinholes of 0.3 mm separated by 7.3 m, and one X-ray source. This provides an X-ray beam that illuminates about a third of the parabola with a divergence less than 15 arcsec. This exercise has been done on MS 58, at 1.5 and 2.2 keV. At 2.2 keV the first and second diffraction order are observed on the same CCD image. The distance between the different energies is the one theoretically expected. These tests allow also to evaluate the energy distribution between the different diffraction orders. The table hereafter, provides a comparison between the measured values and the expected ones^{13,14}. The measurement accuracy is about 1 % (absolute value), the results are close to the expected values.

Table 3: Relative intensity splitting between EPIC focus and diffraction-order foci at 1.5 keV

Unit in %	Measured relative area with respect to EPIC	Theoretical relative area with respect to EPIC
M=0	8	10
M=1	7	9
M=2	3.5	5

8. SLIT TESTS

8.1. Introduction

The slit tests have been introduced, since it is difficult to figure out correct alignment of the individual grating stacks with respect to each other once in operation. The grating stacks were integrated and aligned with interferometric tools, but a full operational test is not possible. Tests were made with an X-ray finite distance point source. Due to this geometry, the RGA is not linked to the MM, and must be aligned several centimeters away from the nominal position of the MM. The advantage of the CSL facility is to provide a perfectly collimated beam illuminating only a stack of gratings (in fact maximum 7 gratings). Due to the high accuracy of the translating table, each stack of grating position will be determined in Y and Z XMM coordinates versus the telescope focus with an accuracy better than 100 μm . This will give the grating stack misalignment with respect to each other. This test is performed before the environmental tests. In case of trouble, the test can be reconducted, and will provide an accurate diagnostic about the impact of the environmental tests on the stack alignment.

8.2. Experimental set-up and results

The experimental set-up consists in using only a small part of the EUV collimated beam, by partially hiding the beam with an Al black anodised plate with a 100 * 95 mm₂ rectangular slit. The MM with the RGA is aligned with respect to this small-collimated beam by maximising the throughput through a dedicated grating stack. The other grating stack positions are known with a sufficient accuracy, so that each grating can be illuminated correctly. This is achieved by translating the MM with the RGA in front of the slit. For each position, the telescope focus is recorded with the EUV facility CCD. Then the CCD is translated towards the 0-order focus. This is performed for the 32 grating stacks and some cross checks are added.

From this data set, the relative positions are evaluated. The figure 9 represents the grating stack displacement with respect to the expected position. The position accuracy is influenced by the tilt of the MM and by the translation table accuracy. For both FM RGA the grating stacks alignment is satisfactory.

For each 0-order position sequence an extrafocal image is recorded. Figure 10 is a recomposition of all the individual extrafocal slit exposure. This figure allows also to detect the defect grating stacks. For several cases it is either possible to discern each grating, and to have data about their orientation.

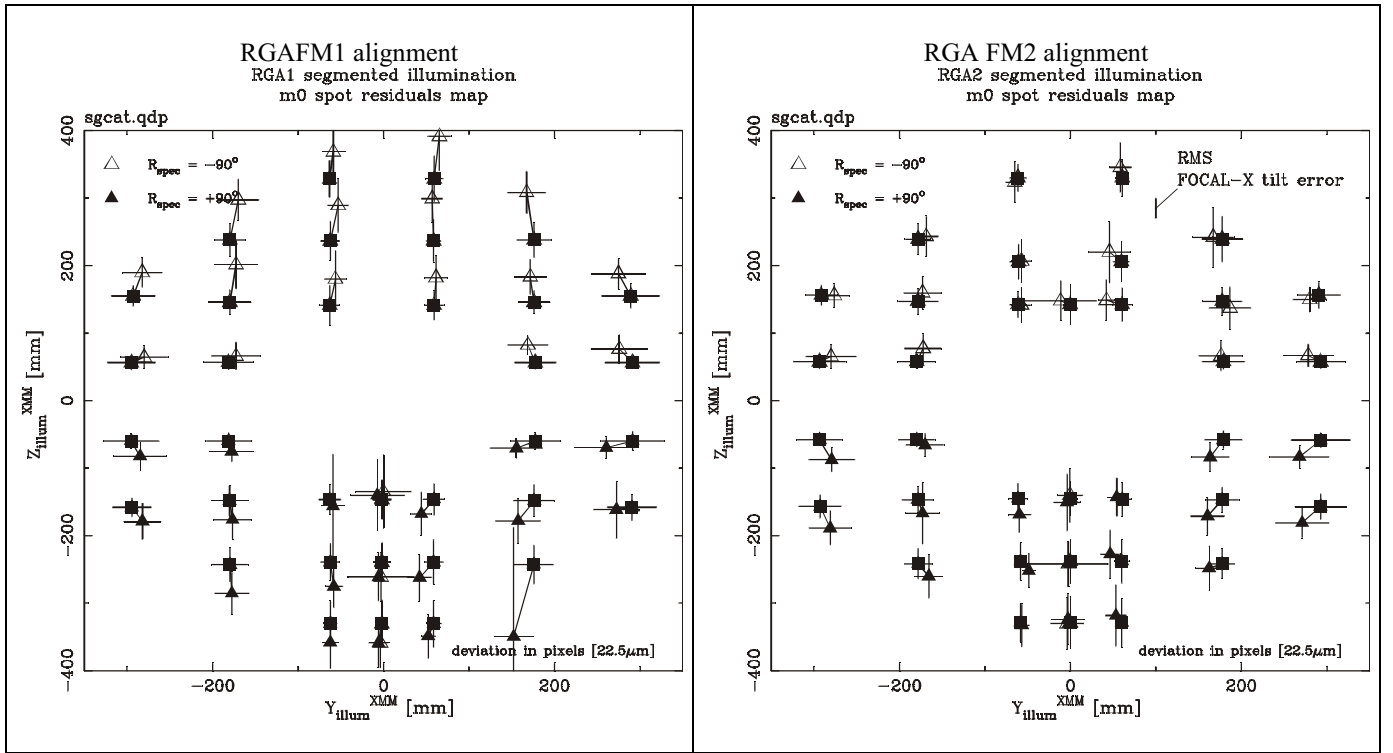


Figure 9: Grating stack position measured at 0-order diffraction.

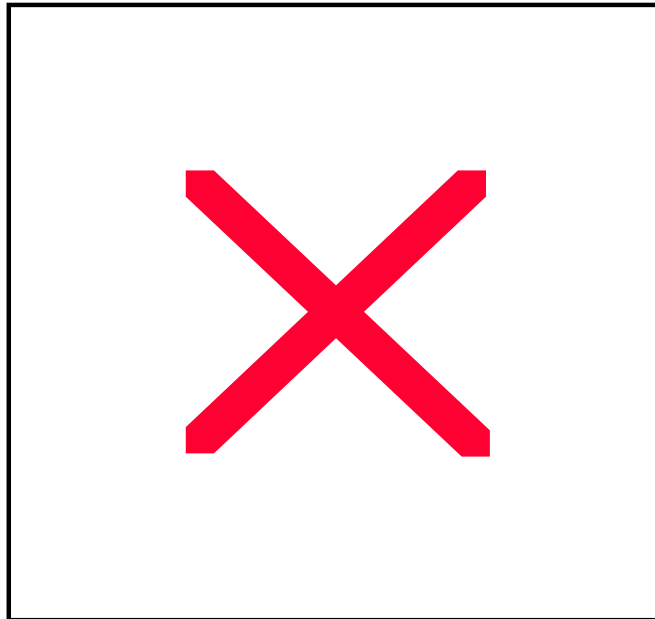


Figure 10 : 0-order Extrafocal recomposition from grating stack illumination.

Individual slit exposure extrafocal images are built into a mosaic representing the grating box, as in the previous figures 7. The transposition of these subimages would resemble the full aperture extrafocal mosaic. This mosaic may be used to identify individual gratings in the array. This image is displayed in logarithmic scale.

9. CONCLUSIONS

For the first time a complete optical Mirror Assembly of the XMM satellite has been tested in flight configuration. A flight Mirror Module equipped with its X-ray baffle and with a Grating Reflecting Assembly has been analysed with a collimated EUV beam. These tests have shown that the environmental tests (thermal and vibration) have no major impact on the image quality neither at telescope focus nor at 0-order focus. It has been confirmed on a small sample that the RGA works correctly in the X-rays once integrated on a MM. The introduction of the RGA increases slightly the HEW at telescope focus, because of diffraction. The energy distribution between the different foci (telescope, 0, 1 and 2 order) fits the expected values. Some complementary tests are planned to be performed on the actual flight combination. These tests will be conducted before the end of this year.

Acknowledgements

Our first thanks go to our colleagues who were able to react in real time and with great care to these new optical tests on flight hardware. Their work is greatly appreciated and is a key factor in the success of these test campaigns on RGA FMs.

In addition we would thanks the XMM Project for the efficient collaboration.

The development of the RGA grating arrays (in the US) is supported by NASA under contract of the University of California at Berkeley, with subcontracts to Columbia University and the Lawrence Livermore National Laboratory.

The vertical facility at CSL was funded by ESA XMM project under the contract number 9939/92/NL/PP.

The XMM FM MM mirrors were replicated and integrated by MEDIALARIO under ESA contract number 0545/93/NL/RE.

References

1. D. de Chambure, R. Lainé, K. van Katwijk, J. van Casteren & P. Glaude, "Producing the X-Ray Mirrors for ESA's XMM Spacecraft", ESA bulletin 89, February 1997
2. F. Jansens, "XMM observatory : a scientific and technical overview", SPIE 3444, San Diego 1998
3. J. van Casteren, "The X-ray multi mirror spacecraft, a large telescope", SPIE 2808 , Denver 1996.
4. Y. Stockman, I. Domken, H. Hansen, J. Ph. Tock, D. de Chambure, P. Gondoin, "XMM Flight Mirror Module environmental and optical testing", SPIE , San Diego 1998.
5. Y. Stockman, J-P. Collette, J. Ph. Tock, "Optical testing of XMM flight model module I and II at the vertical EUV/X facility", SPIE 3114, 566, San Diego 1997
6. J. Ph. Tock, J-P. Collette, Y. Stockman, "Calibration and upgrades of the XMM vertical EUV/X test facility; FOCALX", SPIE 3114, 554, San Diego 1997
7. J. Ph. Tock, J P Collette, I Domken, Ph Kletzkine, Y Stockman, A Vignelles, "FOCAL X : A test facility for X-ray telescopes", 3rd International Symposium on Environmental Testing For Space Programmes, Noordwijk 1997
8. D. de Chambure, K.van Katwijk, R. Lainé, J. van Casteren, G. Peterson, M. Côté, B. Aschenbach, R. Willingale, D. Schink, A. Frey, W. Rühe, Y. Gutierrez, F. Draheim, "Reducing the optical and X-ray stray light in the ESA XMM telescope", ICSO, Toulouse (France), 1997
9. S.M. Kahn, J. Cottam, T.A. Decker, F.B.S. Paerels, S.M. Pratuch, A. Rasmussen, J. Spodek, J.V. Bixler, A.C. Brinkman, J.W. den Herder, C. Erd, "The reflection grating arrays for the reflection grating spectrometer on-board of XMM", SPIE Vol. 2808, 450-462, Denver 1996
10. A.C. Brinkman, H.J.M. Aarts, A.J.F. den Boggende, T. Bootsma, L. Dubbeldam, , J.W. den Herder , J.S. Kaastra, P.A.J. de Korte, B.J. van Leeuwen, R. Newe, E. van Zwet, S.M. Kahn, C.J. Hailey, T.A. Decker, F.B.S. Paerels, S.M. Pratuch, A. Rasmussen, G. Branduardi-Raymont, P. Guttridge, , J.V. Bixler, K. Thomsen, A. Zehnder , C. Erd, "The Reflection Grating Spectrometer on-board of XMM", SPIE Vol. 2808, 463-480, Denver 1996.
11. G. L. Peterson, M. Coté, "Straylight analysis of the XMM telescope", BRO report #3000, Final report 09/30/96.
12. R. Egger, B. Aschenbach, H. Braunerger, W. Burkert, T. Döhring, A. Oppitz, "X-ray calibration of the XMM flight mirror at the Panter test facility", SPIE 3444, San Diego 1998.
13. Frits Paerels, "Effect of the RGA Braces on EPIC and RGS performance", University of Columbia report RGS-COL-CAL-970102, 1997.
14. Jean Cottam, "How to Use the raw efficiency table file", University Columbia report RGS-COL-CAL-970101, 1997.

